Conformational control through cooperative nonconventional C-H···N hydrogen bonds

Eric Boscha\*, Nathan P. Bowlingb and Shalisa M. Oburna

<sup>a</sup>Chemistry Department, Missouri State University, 901 South National Avenue, Springfield,

Missouri, 65897, USA

<sup>b</sup>Department of Chemistry, University of Wisconsin-Stevens Point, 2001 Fourth Avenue, Stevens

Point, WI, 54481, USA

Correspondence email: ericbosch@missouristate.edu

**Synopsis** Cooperative non-conventional  $sp^2$ -C-H···N hydrogen bonds control the conformation of a

dipyridyl molecule to a rhombus shape.

Abstract We report the design, synthesis, and crystal structure of a conjugated aryleneethynyl

molecule, 2-[4,5-dimethoxy-2-(2,3,4-trifluoro-phenylethynyl)-phenylethynyl]-6-pyridin-2-ylethynyl

pyridine, that adopts a planar rhombus conformation in the solid state. The molecule, C<sub>30</sub>H<sub>17</sub>F<sub>3</sub>N<sub>2</sub>O<sub>2</sub>,

crystallizes in space group P-1 with Z = 2 and features two intramolecular  $sp^2$ -C-H···N hydrogen bonds

that cooperatively hold the arylethynyl molecule in a rhombus conformation. The hydrogen atoms are

activated towards hydrogen bonding since they are situated on a trifluorophenyl ring and the H···N

distances are 2.469(16) and 2.646(16) Å with C-H···N angles of 161.7(2) and 164.7(2)° respectively.

Molecular electrostatic potential calculations support the formation of C-H···N hydrogen bonds to the

trifluorophenyl moiety. Hirschfeld surface analysis identifies a self-complementary C-H···O dimeric

interaction between adjacent 1,2-dimethoxybenzene segments that is shown to be common in structures

containing that moiety.

**Keywords:** 

C-H···N hydrogen bonds, intramolecular hydrogen bonding, non-conventional hydrogen bonds,

conformational control, molecular rhombus, self-complementary hydrogen bonds

#### 1. Introduction

The importance of weak hydrogen bonds has long been recognized in crystal engineering (Desiraju & Steiner, 1999 and Domenicano & Hargitta, 2002). One of these weaker interactions is the non-conventional C-H···N hydrogen bond. We previously reported on the dominant role of the  $sp^2$  C-H···N hydrogen bond in the crystallization of a series of (polyfluoro)phenylethynyl pyridines as well as the cocrystallization of a series of bipyridyls with octafluorobiphenyl. (Bosch *et al.*, 2014). Those studies were initiated by the observation of self-complementary  $sp^2$  C-H···N hydrogen bonded dimer formation (Oburn *et al.*, 2015). Others have also reported non-conventional C-H···N hydrogen bonds to polyfluorophenyl containing molecules (Prasang *et al.*, 2013). In that earlier study we also reported two examples of molecules designed to form intramolecular C-H...N hydrogen bonds to facilitate adoption of a planar triangular conformation. Now, we describe an extension of this strategy via the use of two intramolecular C-H···N hydrogen bonds working cooperatively to hold a molecule in a rhombus-shaped conformation.

#### 2. Experimental

### 2.1. Synthesis and Characterization

The synthesis of target compound (1) is outlined in Figure 1. A sequential one-pot palladium catalysed coupling of 2,6-dibromopyridine with one equivalent of 2-ethynylpyridine followed by excess trimethylsilylacetylene yielded a mixture from which a 30% yield of key intermediate (2) was obtained. Base deprotection of (2) followed by Sonogashira coupling with 4,5-diiodoveratrole yielded (3). Sonogashira coupling of (3) with trimethylsilylacetylene followed by deprotection and Sonogashira coupling with 1,2,3-trifluoro-4-iodobenzene formed the target compound (1) in moderate yield.

**Figure 1** Synthetic scheme for the preparation of (1).

# 2.1.1. Synthesis of 2-(2-pyridinethynyl)-6-trimethylsilanylethynyl)pyridine, (2)

Argon was bubbled through a solution of 2,6-dibromopyridine (2.31 g, 9.75 mmol) and 2ethynylpyridine (1.00 g, 9.73 mmol) in triethylamine (20 mL) for 10 minutes before PdCl<sub>2</sub>(PPh<sub>3</sub>) (0.052 g) and CuI (0.012 g) were added. The flask was sealed and stirred at room temperature for 3 days at which time TLC indicated that the 2-ethynylpyridine was consumed. Trimethylsilylacetylene (2 mL, 14 mmol) was added into the reaction mixture and argon bubbled through the mixture for 10 minutes before it was sealed and stirred at room temperature for another 5 days. The reaction mixture was dissolved in dichloromethane and washed with water. The dichloromethane solution was dried over anhydrous magnesium sulphate, filtered and the solvent evaporated under vacuum. The crude product was separated with flash chromatography using mixtures of hexane and ethyl acetate increasing in polarity from 1:1 to 1:4 hexane:ethyl acetate. Compound (2) was isolated as a cream coloured solid (0.81 g, 30 %). <sup>1</sup>H NMR  $(400 \text{ MHz}, \text{CDCl}_3) \delta 8.62 \text{ (md}, J = 4.8 \text{ Hz}, 1\text{H}), 7.75-7.65 \text{ (m, 2H)}, 7.59 \text{ (d, 2H)}$ J = 8 Hz, 1H), 7.54 (d, J = 8 Hz, 1H), 7.43 (d, J = 8 Hz, 1H), 7.30-7.28 (m, 1H), 0.30 (s, 9H). <sup>13</sup>C NMR (100MHz, CDCl<sub>3</sub>)  $\delta$  150.5, 143.8, 143.2, 142.7, 136.9, 136.6, 128.1, 127.34, 127.30, 123.8, 103.4, 95.9, 88.5, 87.7, 0.0. The by-product 2,6-bis-(trimethylsilanylethynyl)pyridine (Heemstra & Moore, 2004) eluted before (2) as a white solid (0.59 g, 22%) while 2,6-bis-(2-pyridinethynyl)pyridine (Potts et al., 1993) eluted after (2) as a light orange solid (1.21 g, 44 %).

# 2.1.2. Synthesis of 2-(2-iodo-4,5-dimethoxy-phenylethynyl)-6-pyridin-2-ylethynyl-pyridine, (3)

Compound (2) was deprotected with KOH (1 equiv) in ethanol (5 mL) and the crude reaction mixture dissolved in dichloromethane and washed with water and brine. The organic solution was dried over sodium sulfate, filtered, and the solvent evaporated under vacuum. The crude product was immediately reacted with an excess (2.0 equiv.) of 4,5-diiodoveratrole according to the procedure described in section 2.1.1. Product (3) was isolated in 62% yield as an off-white solid.  $^{1}$ H NMR (400 MHz, CDCl<sub>3</sub>)  $\delta$  8.65 (d, J = 4.8 Hz, 1H), 7.74-7.69 (tm, J = 8.0 Hz, 1H), 7.76-7.57 (m, 3H), 7.63 (td,

 $J=1.2, 7.8 \text{ Hz}, 1\text{H}), 7.60 \text{ (dd, } J=1.2, 7.9 \text{ Hz}, 1\text{H}), 7.57 \text{ (dd, } J=1.2, 7.8 \text{ Hz}, 1\text{H}), 7.29 \text{ (ddd, } J=1.2, 4.8, 7.2 \text{ Hz}, 1\text{H}), 7.25 \text{ (s, } 1\text{H}), 7.14 \text{ (s, } 1\text{H}), 3.89 \text{ (s, } 3\text{H}), 3.87 \text{ (s, } 3\text{H}).} \ ^{13}\text{C NMR (100 MHz, CDCl}_3) \delta 150.4, 150.3, 149.0, 143.9, 143.0, 142.5, 136.7, 136.4, 127.9, 127.1, 126.9, 123.6, 121.0, 120.8, 115.4, 92.2, 90.6, 90.1, 88.3, 87.6, 56.3, 56.1.$ 

# 2.1.3. Synthesis of 2-[4,5-dimethoxy-2-(2,3,4-trifluoro-phenylethynyl)-phenylethynyl]-6-pyridin-2-ylethynyl-pyridine, (1)

Compound (3) was reacted with a slight excess (1.25 equiv.) of trimethylsilyl acetylene according to the procedure described in section 2.1.1. The trimethylsilyl product was isolated by chromatography and deprotected with 1 eq. KOH in ethanol. The deprotected compound was then reacted with 1.2 eq. of 1,2,3-trifluoro-4-iodobenzene according to the procedure in Section 2.1.1. The product was isolated as a light brown solid (56 %). NMR (400 MHz, CDCl<sub>3</sub>)  $\delta$  8.67 (br d, J = 4.4 Hz, 1H), 7.73-7.69 (m, 2H), 7.61-7.53 (m, 3H), 7.52 (d, J = 8 Hz, 1H), 7.32-7.29 (m, 1H), 7.14 (s, 1H), 7.13-7.06 (m, 1H), 7.04 (s, 1H), 3.95 (s, 3H), 3.93 (s, 3H).  $^{13}$ C NMR (100 MHz, CDCl<sub>3</sub>)  $\delta$  151.4 (dddd, J = 250, 25, 10, 3 Hz, 150.4, 150.0, 149.7, 144.1, 143.2, 142.7, 140.7 (td, J = 251.1, 15.2 Hz), 136.7, 136.5, 132.2 (d, J = 9.9 Hz), 132.1 (d, J = 2.3 Hz), 128.7 (d, J = 12.2 Hz), 128.0 (dd, J = 6.8, 3.8 Hz), 127.9, 126.9, 126.8 (d, J = 1.5 Hz), 132.7, 118.9, 118.1, 114.7, 114.1, 111.4 (ddd, J = 287.7, 18.3, 3.8 Hz), 94.0 (dd, J = 3.7, 2.3 Hz), 91.5, 88.6, 88.2, 87.8, (dd, J = 3.7, 2.4 Hz), 56.3.

### 2.2. Refinement

A single crystal of (1) was mounted on a Kryoloop using viscous hydrocarbon oil. Data were collected using a Bruker Apex1 CCD diffractometer equipped with Mo K $\alpha$  radiation with  $\lambda$  = 0.71073 Å. Data collection at low temperature was facilitated by use of a Kryoflex system with an accuracy of  $\pm 1$  K. Initial data processing was carried out using the Apex II software suite (Bruker, 2014). Structures were solved using the dual-space method SHELXT-2018 (Sheldrick, 2015a) and refined against F<sup>2</sup> using SHELXL-2018 (Sheldrick, 2015a). The program X-Seed was used as a graphical interface (Barbour, 2020). All H atoms were located in the difference maps. The hydrogen atoms involved in C-H···N hydrogen-bonding interactions were restrained in the refinement with C-H = 0.95(2) Å and with Uiso(H) = 1.2Ueq(C). All other hydrogen atoms were treated as riding atoms in geometrically idealized positions with C-H = 0.95 Å and Uiso(H) = 1.2Ueq(C). The crystallographic data are collected in Table 1. Crystal data, data collection and structure refinement details are summarized in Table 1 and hydrogen bond parameters are collected in Table 2.

## 2.3. Electrostatic potential and Hirschfeld surface calculations

The molecule 4-(phenylethynyl)-1,2,3-trifluorobenzene was geometry optimized with density functional theory (DFT) at the B3LYP/6-311+G\*\* level, and the corresponding molecular

electrostatic potential energy surface calculated using Spartan'10 (Wavefunction, 2010). The program CrystalExplorer 2017 was used to calculate the Hirschfeld surface (Turner *et al.*, 2017).

#### 3. Results and discussion

The asymmetric unit of the X-ray structure of (1) contains a single molecule in the closed rhomboidal conformation with two intramolecular C-H···N hydrogen bonds as shown in Figure 1. The molecule (1) is essentially planar with the pyridyl ring N1-C5 slightly twisted out of the plane defined by the two benzene rings and pyridine C8-N2 with an interplanar angle between the two pyridyl rings of 6.85 (9)°. Specifically, atoms N1, C1 and C2 are 0.448(2), 0.534(3) and 0.444(3) Å above the plane defined by the atoms in the other three aromatic rings. For comparison, the root mean square deviation of the fitted atoms is 0.040 Å with a maximum deviation of 0.102(2) for C28.

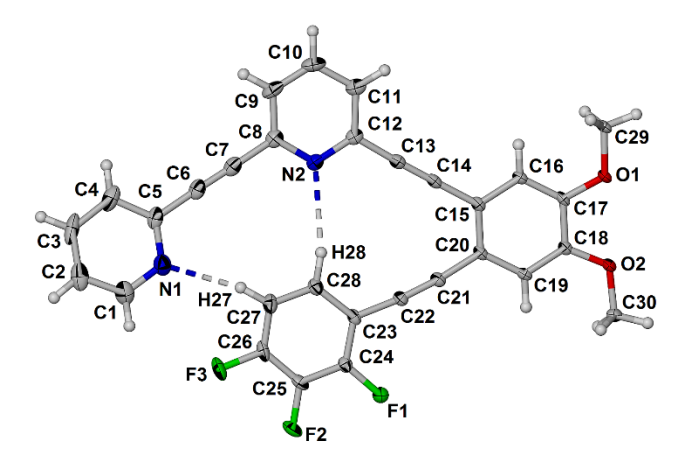


**Figure 2** Labelled asymmetric unit of (1) showing the two phenyl  $sp^2$ -C-H···N hydrogen bonds as dashed lines. Displacement ellipsoids drawn at the 50% level.

The interaction C27-H27···N1 has C···N and H···N distances of 3.400 (3) and 2.469 (16) Å, 90% of the sum of the van der Waals radii of 2.75 Å (Bondi, 1968), while the second interaction has C28···N2 and H28···N2 distances of 3.61 (2) and 2.646 (16) Å, 97% of the sum of the van der Waals radii. The two hydrogen bonds have C27-H27···N1 and C28-H28···N2 angles of 161.7 (2) and 164.7 (2) respectively. While a calculation of the molecular electrostatic potential of (1) in the hydrogen bonded rhomboid conformation would not provide information related to the relative hydrogen bond donor capability of the trifluorophenyl moiety we reasoned that the molecular electrostatic potential of 2,3,4-trifluorotolane would be more informative. Indeed, the molecular electrostatic potential shown in Figure 3 amplifies the ditopic hydrogen bond donor potential of this moiety. The maximum electrostatic potential on the H atoms corresponding to H27 and H28 are 136.3 and 129.3 kJ/mol

respectively as compared to the potential of 170.4 kJ/mol on the proton in pentafluorobenzene calculated in the same way.

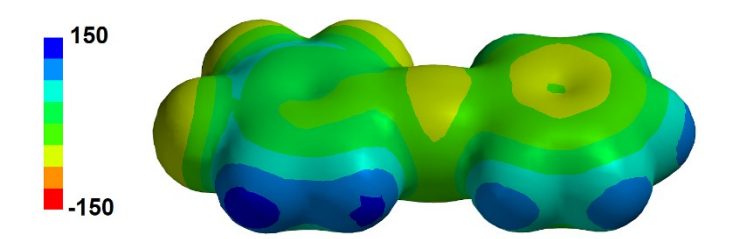


**Figure 3** The molecular electrostatic potential map of 2,3,4-trifluorotolane with colour coded legend from -150 to 150 kJ/mol.

A Hirschfeld surface plot was calculated to investigate intermolecular interactions within the crystalline structure. The surface is shown in Fig. 4 with red areas indicating especially close contacts to adjacent molecules.

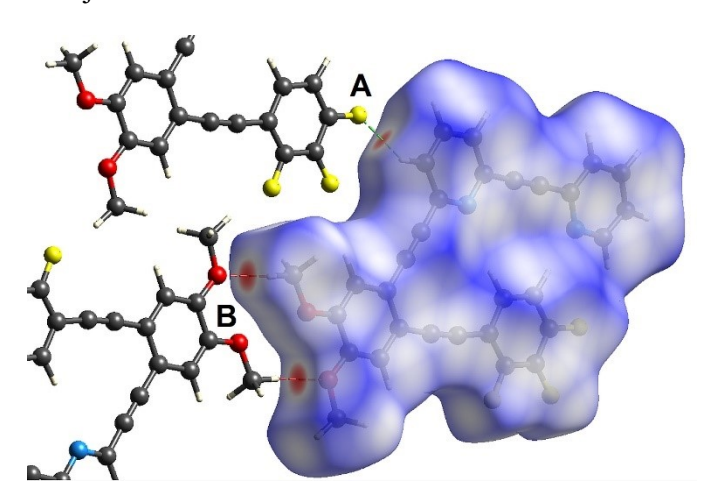


**Figure 4** Hirshfeld surface of (1) showing close intermolecular contacts  $\mathbf{A}$  (C-H···F) and  $\mathbf{B}$  (C-H···O) as red areas.

The intermolecular contact **A** is a C-H···F interaction that features C11···F3<sup>i</sup> (symmetry code: (i) x, y+1, z) and H11···F3<sup>i</sup> distances of 3.221 (3) and 2.41 Å (93 % of the sum of the van der Waals radii) respectively and a C11-H11···F3<sup>i</sup> angle of 146.5(2)°. Contact **B** corresponds to a self-complementary methyl C-H···O interaction, C-H29B···O2<sup>ii</sup> (symmetry code: (ii) -x+3, -y+2, -z+1), with C29···O2<sup>ii</sup> and H29B···O2<sup>ii</sup> distances of 3.350 (2) and 2.37 Å (86% of the sum of the van der Waals radii). The C29-H29B···O2<sup>ii</sup> angle is 175°.

The molecules of (1) pack side-by-side in the crystal to form planar sheets shown in Fig. 5.

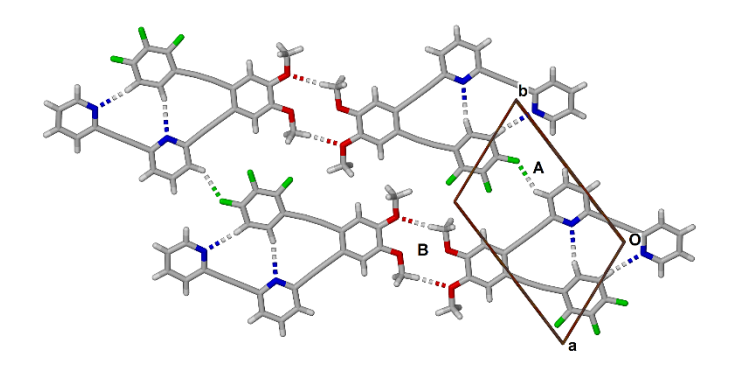


**Figure 5** View of a plane of molecules (1) viewed along the c axis with intermolecular interactions labelled **A** and **B**.

A search of the Cambridge Crystallographic Database (Version 5.41, update of March 2020; Groom *et al..*, 2016) using *Conquest* (Bruno *et al..*, 2002) for structures including the C-H···O hydrogen bonded dimer synthon as shown in Fig. 6 (a), with both C-H···O distances equal to, or less than, the sum of the Vander Waals radii, yielded 806 hits. A modified search revealed that 639 hits corresponded to 1,2-dimethoxy benzene derivatives shown in Fig 6(b). For context, a search for organic structures including the 1,2-dimethoxy benzene moiety yielded a total of 5651 hits. Therefore, the self-complementary interaction shown in Fig. 6(b) is common occurring in 11.3% of structures that include the dimethoxy veratrole moiety irrespective of other substitution patterns.

**Figure 6** (a) Self-complementary CH···O (ether) hydrogen bonded dimer scheme used in the CSD Conquest search and (b) modified criteria for compounds containing the 1,2-dimethoxybenzene moiety.

## 4. Conclusions

We have demonstrated that cooperative non-conventional C-H···N hydrogen bonds effectively control the conformation of 2-[4,5-dimethoxy-2-(2,3,4-trifluoro-phenylethynyl)-phenylethynyl]-6-pyridin-2-ylethynyl-pyridine resulting in the formation of a planar rhombus molecular conformation. The self-complementary C-H···O hydrogen bonding interaction between 1,2-dimethoxy benzene moieties identified in the structure has been shown to be common and may have application in supramolecular chemistry.

**Acknowledgements** We thank the National Science Foundation for financial support of this research (RUI Grant No. CHE-1903593).

#### References

Barbour, L. J. (2020). J. Appl. Cryst. 2020, 53, 1141-1146.

Bondi, A. (1964). J. Phys. Chem. 68, 441-451.

Bosch, E., Bowling, N. P. & Darko, J. (2015). Cryst. Growth & Des. 15, 1634-1641.

Bruker (2014). SMART, SAINT and SADABS. Bruker AXS Inc., Madison, Wisconsin, USA

Bruno, I. J., Cole, J. C., Edgington, P. R., Kessler, M., Macrae, C. F., McCabe, P., Pearson, J. & Taylor, R. (2002). *Acta Cryst.* **B58**, 389–397.

Desiraju, G. R. & Steiner, T. (1999). *The Weak Hydrogen Bond: In Structural Chemistry and Biology*. Oxford University Press.

Domenicano, A. & Hargitta, I. (2002). Strength from Weakness: Structural Consequences of Weak Interactions in Molecules, Supermolecules, and Crystals, Springer.

Groom, C. R., Bruno, I. J., Lightfoot, M. P. & Ward, S. C. (2016). Acta Cryst. B72, 171–179.

Heemstra, J. M. & Moore, J. S. (2004). Org. Lett., 6, 659–662.

Potts, K. T., Horwitz, C. P., Fessak, A., Keshavarz-K, M., Nash, K. E. & Toscano, P. J. (1993) *J. Am. Chem. Soc.* **115**, 10444-10445.

Oburn, S. M., Bowling, N. P. & Bosch, E. (2015) Cryst. Growth Des., 15, 3, 1112–1118.

Prasang, C., McAllister, L. J., Whitwood, A. C. & Bruce, D. W. (2013) CrystEngComm, 15, 8947–8958.

Sheldrick, G. M. (2015a). Acta Cryst. A71, 3–8.

Sheldrick, G. M. (2015b). Acta Cryst. C71, 3–8.

Turner, M. J., Mckinnon, J. J., Wolff, S. K., Grimwood, D. J., Spackman, P. R., Jayatilaka, D. & Spackman, M. A. (2017). *CrystalExplorer17*. The University of Western Australia.

Wavefunction (2010). Spartan'10. Wavefunction Inc., Irvine, CA, USA.

# Table 1 Experimental details.

(1)

Crystal data

Chemical formula C<sub>30</sub>H<sub>17</sub>F<sub>3</sub>N<sub>2</sub>O<sub>2</sub>

 $M_{\rm r}$  494.45

Crystal system, space group Triclinic,  $P^-1$ 

Temperature (K) 100

a, b, c (Å)8.0037 (4), 12.1365 (6), 13.4922 (6)α, β, γ (°)104.697 (1), 103.023 (1), 106.619 (1)

 $V(Å^3)$  1150.30 (10)

Z 2

Radiation type Mo  $K\alpha$  $\mu \text{ (mm}^{-1}\text{)}$  0.11

Crystal size (mm)  $0.56 \times 0.23 \times 0.21$ 

Data collection

Diffractometer Bruker APEX-I CCD

Multi-scan

Absorption correction SADABS V2014 (Bruker, 2014)

 $T_{\min}, T_{\max}$  0.714, 0.746

No. of measured, independent

and

observed  $[I > 2\sigma(I)]$  14094, 5017, 3939

reflections

 $R_{\text{int}}$  0.022  $(\sin \theta/\lambda)_{\text{max}} (\mathring{A}^{-1})$  0.642

Refinement

 $R[F^2 > 2\sigma(F^2)], wR(F^2), S$  0.050, 0.137, 1.04

No. of reflections 5017

No. of parameters 342

No. of restraints 2

H-atom treatment

H atoms treated by a mixture of independent and constrained

refinement

 $\Delta \rho_{\text{max}}, \Delta \rho_{\text{min}} (e \text{ Å}^{-3})$  0.62, -0.28

 Table 2
 Selected hydrogen bond parameters.

| D— $H$ ··· $A$              | <i>D</i> —H (Å) | $\mathbf{H}\cdots A$ (Å) | $D\cdots A$ (Å) | D— $H$ ··· $A$ (°) |
|-----------------------------|-----------------|--------------------------|-----------------|--------------------|
| C11—H11····F3 <sup>i</sup>  | 0.95            | 2.41                     | 3.220 (2)       | 142.5              |
| C27—H27···N1                | 0.966 (16)      | 2.470 (17)               | 3.400 (3)       | 161.7 (19)         |
| C28—H28···N2                | 0.991 (15)      | 2.646 (16)               | 3.612 (2)       | 164.7 (17)         |
| C29—H29B···O2 <sup>ii</sup> | 0.98            | 2.37                     | 3.350(2)        | 174.8              |

Symmetry code(s): (i) x, y+1, z; (ii) -x+3, -y+2, -z+1.